Proceedings of The Fourteenth (2004) International Offshore and Polar Engineering Conference
Toulon, France, May 23–28, 2004

ISBN 1-880653-62-1 (Set); ISSN 1098-6189 (Set)

Wave Spectra from ENVISAT's Synthetic Aperture Radar in Coastal Areas

F. Ardhuin(1), F. Collard(2), B. Chapron(3)

1. Centre Militaire Océanographique, Service Hydrographique et Océanographique de la Marine. Brest, France

2. Boost Technologies Plouzané, France

3. IFREMER, Centre de Brest Plouzané, France

ABSTRACT

A field experiment was carried out on the French coast of the English channel to investigate the tidal modulation of ocean waves. Swell condition dominated the one month measurement campaign. In-situ measurements of wave spectra by 7 sensors are compared to spectra derived from a Synthetic Aperture Radar image acquired by ENVISAT's ASAR instrument. The wave spectra inversion scheme is adapted for shallow water from ESA's operational processing techniques used for level 2 ocean wave products. For low to moderate wind speeds good agreement is found between in-situ and SAR observations, over a wide range of wave heights and directions, including waves propagating in the radar azimuth direction.

KEY WORDS: Waves; SAR; coastal; ENVISAT.

INTRODUCTION

The knowledge of wave conditions, either as climatology or short term forecast is critical for all human activities at sea, including shipping, fishing, oil extraction and naval operations. The development of wave models has been very fruitful over the past few decades and wave forecasts are now quite reliable in the open ocean. Because wave models compute the wave field from surface winds, often provided by atmospheric models, this progress was made possible by advances in weather forecasting and remote sensing of winds over the oceans. This reliability of wave models have been established thanks to wave height measurements with space-borne range altimeters, as well as the exchange of in-situ observation from wave buoys. Current efforts to improve global wave forecasting is now limited by the poor availability of spectral wave measurements that can discriminate in details the good and not so good parameterizations. Synthetic Aperture Radar 'imagettes' have now been acquired routinely since 1992, covering small areas (imagettes were 10 by 5 km) of the ocean surface by ERS 1 and 2 and now ENVISAT. These data are still little used because of limitations in the weather conditions under which a wave spectrum can be retrieved from the image. The use of SAR imagettes for assimilation to improve wave models has also been reduced by the vast improvements in wave forecasting.

However, the processing of SAR images has also progressed, and, surprisingly the use of SAR images for ocean waves in coastal areas has been extremely limited in spite of general larger model errors and poor knowledge of wave conditions. SARs, and in particular ENVISAT's Advanced SAR (ASAR), have a unique potential for imaging large areas, providing information on the spatial variations of the wave field, even if SAR is generally limited to the measurements of long waves, which is not relevant in enclosed seas.

We describe here the extension to coastal areas of an algorithm designed for wave spectra estimation from single look complex (SLC) SAR images, and some first validations.

WAVE MEASUREMENT BY SAR

Inversion principles

Synthetic aperture radars rely on the deplacement of the antenna (e.g. with a satellite) to provide a fine resolution in the flight (azimuth) direction that could only be achieved by fixed antennas with a much lager aperture. This precise determination of the origin of echoes in the azimuth direction is given by the Doppler shift of the scattered signal. Resolution in the range direction is given by usual range-gating of the return signal. Therefore the echo of a fixed scatterer at the ocean surface can be transformed into a pixel on the SAR image. This image is formed by mapping the intensity of the backscattered signal in physical space, assuming that scatterers are not moving. Because the ocean surface does move, the SAR image thus shows the scatterers not at their true position in physical (*x*-*y*) space but rather at their position in `range-Doppler' space.

The electromagnetic (E.M.) waves are scattered and reflected by the ocean surface with an intensity that is related to the orientation of the ocean surface, over scales larger than the E.M. wavelength λ, and the roughness of the surface at the scales comparable to λ. In C-band $\lambda \approx 2$ cm, so that ocean waves can be seen because of several imaging processes:

(i) the wind sea and swell modulates the amplitude of the (short) capillary waves, and thus the backscatter intensity (hydrodynamic modulation)
(ii) the wind sea and swell modulates the slope of the sea surface (tilt modulation)
(iii) the wave orbital velocity, with surface convergence and divergence, results in a wavy pattern in the image as the scatterers moving on the waves are placed according to their Doppler velocity (this is known as velocity bunching).

The wavy pattern on SAR images is generally described by its 2D wavenumber spectrum, which is related to the ocean surface elevation (wave) spectrum. After many developments, a certain consensus has been reached on the SAR imaging mechanisms of the ocean surface waves, and its limitations, and a theory is available for simulations of SAR spectra from real ocean wave spectra (Krogstad 1992). Velocity bunching is clearly recognized to be the dominant modulation mechanism, and it is very well described by theory. Besides this, hydrodynamic modulation theories give still unsatisfactory descriptions of the scatterers distribution over the longer wave profile and will be neglected here. For low incidence angles, the tilt modulation is also thought to dominate the hydrodynamic modulation.

Based on theoretical relations giving SAR spectra from wave spectra, as a non-linear analytical expression, different algorithms have been developed for inverting the wave spectrum from an observed SAR spectrum. A retrieval algorithm generally attempts to reconstruct the ocean wave spectrum by minimizing the difference between its corresponding theoretical SAR spectrum (obtained with a forward transformation) and the satellite observation. The exact derivative of the nonlinear transform being too cumbersome to carry out, most of the inversion schemes partially ignore the complete non-linear mapping and mostly use the simplifying gradient of a so-called optimised SAR quasi-linear transform that best matches the full non linear transform (Hasselmann and Hasselmann 1991). The first detailed evaluation of the ERS-1 SAR Wave Mode based on this inversion methodology was performed for a 3-day dataset in the Atlantic Ocean (Bruening et al 1994). Improvements to this technique have focused on a better partitioning of the first guess wave spectral information (e. g. Hasselmann et al. 1996).

The approach used in the present paper was designed to avoid the need for a first guess. This inversion is done in two steps: one for the wind sea part of the spectrum, the other for the swell. The first step uses the complete nonlinear SAR forward transform starting from an a priori knowledge of the wind speed (Mastenbroek and De Vaalk 2000). Subsequently, the minimization is done over the two main parameters governing the wind sea: the sea state degree of development and the mean propagation direction. The necessary a priori wind sea spectrum can be the result of a known local wind vector (measurement or numerical model output). In the second step, the swell spectrum is directly estimated from the residual signal, i.e. the observed SAR spectrum minus the wind sea contribution evaluated in step 1. To further simplify the inversion, step 2 can be done by assuming a linear mapping. To ensure the validity of the inversion, this two-step scheme is iterated. Concerning the 180° ambiguity in the swell propagation direction, an a priori guess spectrum model output and/or the result of a cross-spectral analysis when SAR single-look complex products are available can be used.

Description of the algorithm

We use here the algorithm used to produce level 2 wave spectra products from ESA's ENVISAT ASAR imagettes, slightly modified to accommodate shallow water effects. This wave spectrum retrieval scheme involves two main steps: one for the identification of the purely nonlinear contribution, the other for the swell only contribution. After identification and estimation of the nonlinear contribution to the observed cross-spectrum (i.e. mostly the wind sea contribution), a residual SAR spectrum is computed from the subtraction between the observed spectrum and this nonlinear contribution. The obtained remaining spectrum is then solely a quasi-linear contribution which can easily be solved with respect to the swell spectrum after proper estimation of the linear modulation transfer function (RAR MTF) and the azimuth cut-off parameter.

The retrieval methodology starts by pre-processing the SLC data to perform the "look" extraction and the cross spectral estimation. This pre-processing stage follows the dsteps listed below:

(i) Detrend the input SLC image using a Gaussian low pass filter operation where the width of the filter is set such as to remove the low frequencies not related to waves.
(ii) Compute the co-spectrum and the two cross-spectra corresponding to three looks.
(iii) Estimate the system transfer function, the bias of the co-spectra and remove it from the co-spectra.

This procedure gives one unbiased co-spectra and two cross spectra generated with different look separation times. All of these spectral estimates are combined statistically and used in the wind and wave spectra retrieval.

For the wind retrieval part, both the spectral and the phase information of the cross spectra are combined with the radar cross section (obtained after properly calibrating the image intensity). The wind retrieval methodology then follows:

(i) Estimate the azimuth cut-off factor by fitting cross-spectra to look-up table
(ii) Fit the phase measurements to the look-up table with respect to wind direction
(iii) Use the wind direction, the measured radar cross section, and empirically derived backscatter model function (CMOD) to estimate the wind speed
(iv) Alternatively or in addition, the azimuth spectral time decorrelation can be estimated from azimuth spectral ratios of spectra with different look separation times (0, τ, and 2τ). These measures can also be combined with the look-up table to yield wind speed estimates.

The next step is the determination of a wave spectrum from the image. The fundamental assumption is that the cross spectral transform can be expressed as the sum of a nonlinear part and a quasi-linear part. The different steps of the wave spectrum retrieval procedure are:

(i) Use the estimated wind field to extract the non-linear spectral part, the azimut cut-off factor, and the MTF, from the look-up table.
(ii) Remove the non-linear contribution and solve for the symmetric and asymmetric wave spectra for co- and cross-spectra.
(iii) Compute weighted average solutions for symmetric and asymmetric spectra using the clutter noise values.
(iv) Compute the SNR of the asymmetric spectra.
(v) If the SNR is above certain threshold, then smooth the asymmetric spectra (SNR dependent), and combine the symmetric and asymmetric wave spectra using their clutter noise levels to yield the ambiguity free wave spectrum.
(vi) If SNR is below a certain threshold no ambiguity removal is

performed and the symmetric spectrum is kept unchanged.

The swell inversion procedure will estimate the swell wave spectrum resolved by the SAR (the detected wavy pattern in the SAR scene). Note that, although the extraction of the swell is based on the quasi-linear transform, the inversion use the full theoretical nonlinear SAR mapping through the coupling with the nonlinear part.

The algorithm described above has been developed originally for the wave inversion of ENVISAT ASAR wave mode as a unique incidence angle and assuming infinite depth. The SAR products used here for validation are the complex single look complex image mode where the incidence vary from 15 to 40 degrees and in coastal areas, the deep water assumption is no longer valid. The inversion algorithm has therefore been generalized in two ways. First, the SAR modulation transfer function (MTF) accounting for short wave tilted by larger waves has been generalized to take into account the local variation of backscatter around the changing incidence angle. This was simply implemented by applying for all incidence angles the CMOD empirical relationship relating incidence to C-band backscatter. Second, the surface orbital velocities for a given wavenumber, entering the velocity bunching MTF, have been modified taking into account the linear dispersion relation for surface gravity waves $\omega^2=gk \tanh(kh)$, applicable to any water depth h , with g the acceleration of gravity and k and ω the wavenumber and radian frequency of the waves, respectively. This replaces the deep water limit $\omega^2 = gk$.

Since the SAR determines a wavenumber spectrum, transformation to frequency-direction spectra must of course use the general dispersion relation. Effects of stronger non-linearity and changes in the hydrodynamic modulation transfer function may impact the SAR image analysis and are not considered here. The inversion algorithm has not been tuned in any way to the observations.

VALIDATION OF SAR INVERTED SPECTRA IN COASTAL AREAS

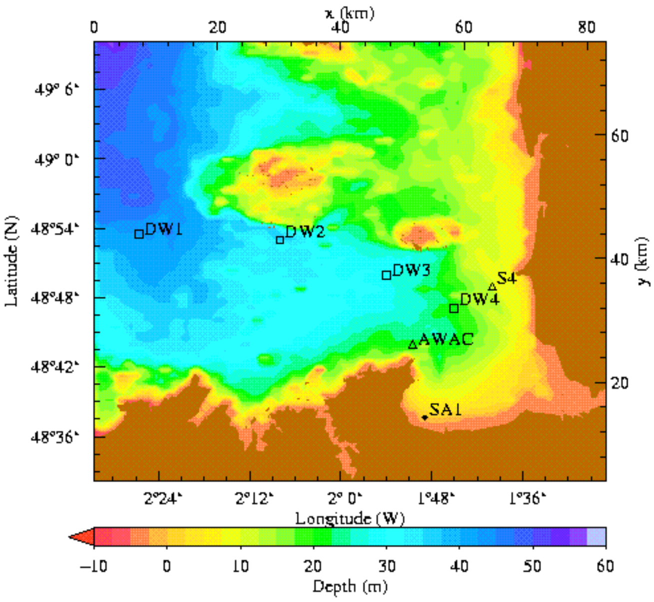

Fig.1: Bathymetry and position of the in-situ instruments.

Observation were obtain as part ot the 'EPEL-2003' campaign initially designed for the validation of wave models in strong tidal environments (organized by SHOM and CETMEF). This was conducted in parallel of a campaign of shallower water measurements by Ifremer and University of Caen. The area where measurements were performed is under the influence of North Atlantic swells, and strong tides (typical tidal range is 10 m, with currents often over 1 m/s).

The In-situ data reported here were obtained with 4 Datawell Waverider buoys (2 being directionals, DW1 and DW4, DW3 and DW2, measured heave only), one Nortek AWAC wave-current profiler, one Interocean S4DW wave-current meter, and a tripod (SA1) equipped with a Paroscientific pressure gauge and an electromagnetic MarshMcBirney current-meter. All these instruments were deployed in the Golfe Normand-Breton, in the western English Channel, between Saint Malo and Granville, in water depths from 30 to 6 m (at high tide), with a typical tidal range of 10 m (figure 1).

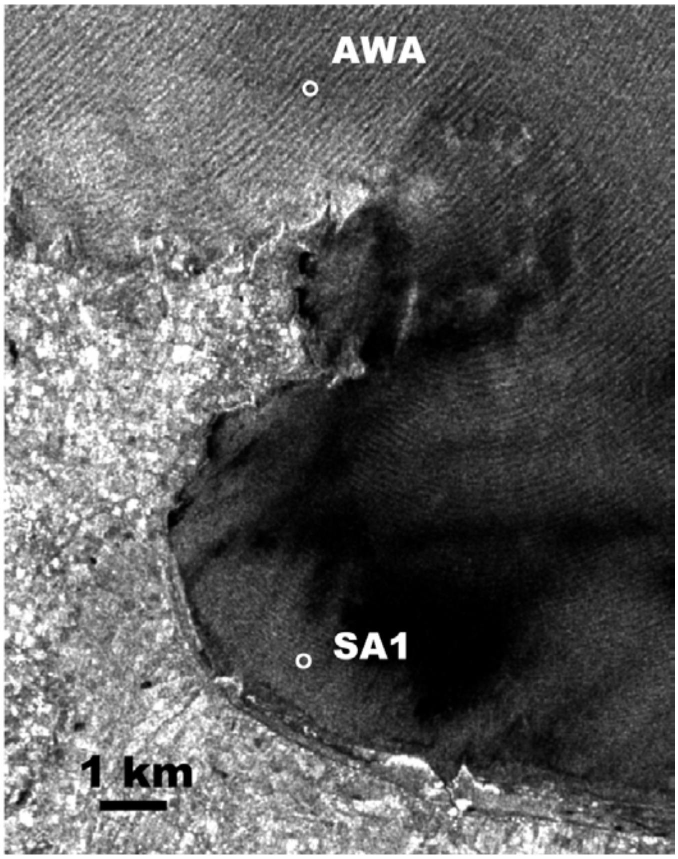

Fig. 2 Excerpt of the image acquired by ENVISAT on March 9 2003 at 21h45. The position of two instruments is indicated. The dark areas correspond to regions of very weak winds. The refraction of waves around the Pointe du Grouin is clearly visible.

A total of 7 ASAR SLC products were delivered by ESA, corresponding to images acquired on February 24, March 6 and 9. Out of these, only 3 contained good wave information, and were acquired on March 9 at 10h22 UTC and 21h44 UTC, and two of these are consecutive along the same orbit.

Wave spectra inversion was performed from 2 km by 2.5 km imagettes in the azimuth and range directions, respectively, corresponding to 512 by 128 SAR pixels, giving a wave spectrum every 2 km. Here we present comparisons of wave parameters obtained from the 2 images acquired in the morning of 9 March and the one acquired in the evening, at the locations close to the in-situ measurements. Due to the analysis technique, the distance between the measurement point and the spectral estimation is at most 1.7 km.

Both images were acquired close to high tide, with relatively weak currents present.

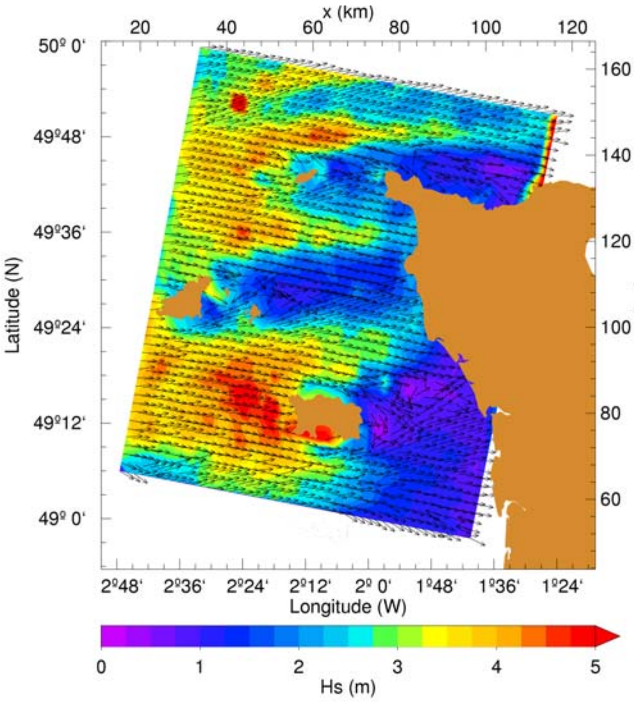

Figure 3: Wave heights and mean wave propagation direction obtained from the 10h24 image.

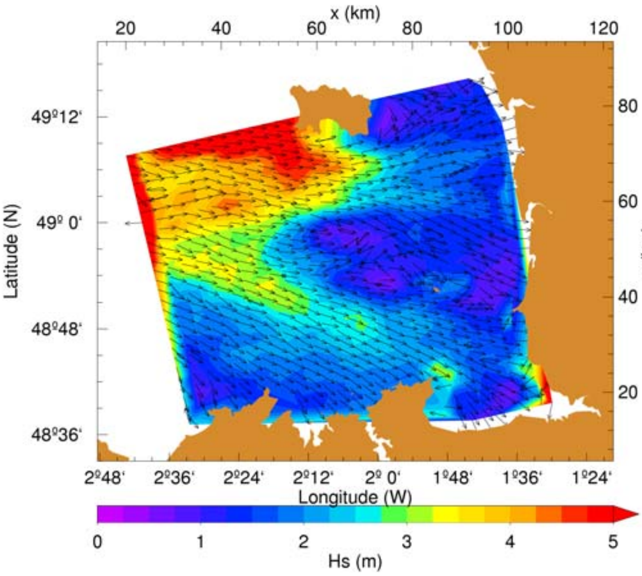

Figure 4: Wave heights and mean wave propagation direction obtained from the 21h44 image.

The variation of wave height in space shows the sheltering effets of islands, high shoals (the central area of figure 3 corresponds to the Minquiers shoals), and headlands. These patterns closely resemble what can be obtained by numerical wave modeling.

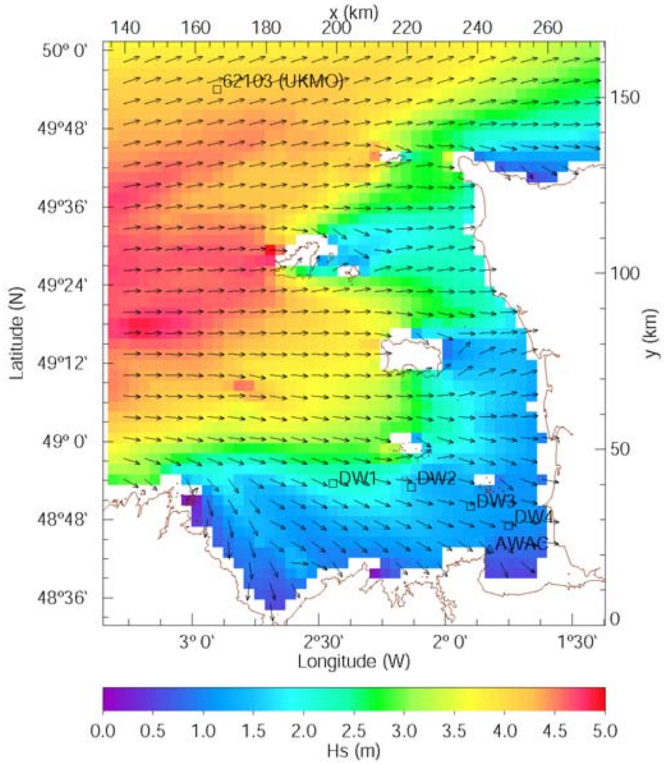

Figure 5: Numerical simulation of waves at 21h44 using the model Wavewatch III, version 2.22 (Tolman 2002), forced by north Atlantic swell 0-24 h forecasts (provided by NOAA/NCEP), high-resolution winds (Météo-France) and tidal currents and water levels (Ifremer).

In spite of the limited area covered by each image, the map of Hs obtained appear to be rather smooth. A detailed estimation of theoretical uncertainties on the SAR spectra and Hs estimates, related to signal to noise ratio in the image and the random nature of wave trains will be described elsewhere and has not been determined yet.

We now compare SAR-derived parameters to in-situ data.

Site:	DW1	DW2	DW3	DW4	AWA	S4	SA1
Depth (m):	49	41	34	25	27	15.4	7.1
In-situ Hs	2.35	0.90	1.14	1.08	1.23	0.84	0.31
SAR Hs (m)	2.38	0.93	0.99	0.92	1.62	N.A.	N.A.
In-situ fp	0.071	0.078	0.085	0.071	0.071	0.077	0.082
SAR fp (Hz)	0.074	0.093	0.095	0.091	0.088	N.A.	N.A.
In-situ θp	292°	N.A.	N.A.	287°	300°	278°	15°
SAR θp	307°	276°	278°	280°	298°	N.A.	N.A.
In-situ $\sigma_{\theta p}$	13°	N.A.	N.A.	14°	26°	26°	9°
SAR $\sigma_{\theta p}$	15°	22°	41°	36°	25°	N.A.	N.A.

Table 1: Wave parameters for 9 March 2003, 10h22 UTC.

Site:	DW1	DW2	DW3	DW4	AWA	S4	SA1
Depth (m):	49	41	34	25	27	15.1	5.51
In-situ Hs	3.05	0.98	1.22	1.27	1.54	0.99	0.66
SAR Hs (m)	3.15	1.70	1.95	1.63	2.35	1.25	0.97
In-situ fp	0.066	0.078	0.078	0.070	0.061	0.070	0.077
SAR fp (Hz)	0.081	0.068	0.11*	0.071	0.078	0.095	0.067
In-situ θp	294°	N.A.	N.A.	282°	305°	276°	14°
SAR θp	287°	283°	280°	286°	303°	270°	25°
In-situ $\sigma_{\theta p}$	13°	N.A.	N.A.	18°	24°	27°	5°
SAR $\sigma_{\theta p}$	7°	22°	31°	9°	23°	42°	39°

Table 2: Wave parameters for 9 March 2003, 21h44 UTC. (*)this high peak frequency corresponds to a spurious second peak in the spectrum (the lowest peak is at 0.09 Hz).

SAR spectra were restricted to wavelength longer than 100 m. In general the wave height and direction is well estimated and directional spectra have a reasonable swell shape. However, at the shallowest site (SA1), the spectrum shows a large component travelling against the observed swell direction, possibly due to the the very inhomogeneous wind speed within this imagette : the wave induced backscatter intensity modulation is here dominated by the small scale wind induced backscatter intensity modulation. In this case the cross-correlation technique has difficulties resolving the propagation direction. Further, the swell peak are generally well represented in the SAR-derived spectra but higher frequency show some occasional large discrepancies with observations.

CONCLUSIONS

The analysis of SAR images can yield a large amount of information for coastal applications, including wave spectra and their variation in space. The straightforward adaptation of the ENVISAT ASAR level 2 algorithm to the processing of narrow swath images was described here. Comparison with in-situ data reveal a general good description of swell propagation close to the coast, including waves propagating in the radar azimuth direction, with wavelength down to 100 m and less. Frequency spectra shapes are generally not well represented at frequencies above twice the peak frequency. The relative low level of noise in SAR-derived maps of significant wave height is encouraging for higher resolution processing in order to obtain directional information. However, the estimation of wave height will still be limited by random wave variations on the scale of wave groups.

ACKNOWLEDGEMENTS

In-situ data was acquired thanks to the contribution of CETMEF and the dedication of the crew and divers from the R/V *Laplace* and Mission Hydrographique de l'Atlantique. We are thankful to ESA for providing ENVISAT images, and Pierre Le Hir for the SA1 in-situ measurements.

REFERENCES

Alpers, W.R., and C. Brüning, 1986, On the relative importance of motion-related contributions to the SAR imaging mechanism of ocean surface waves,*IEEE Trans. Geosci. And Remote Sens.*, **GE-24**(6),873-885.

Brüning, C., S. Hasselmann, and K. Hasselmann, 1994, First evaluation of ERS-1 synthetic aperture radar wave mode data, *Global Atmos. Ocean Syst.*, **2**, 61-98.

Engen, G. and H. Johnsen, 1995, SAR-Ocean wave inversion using image cross-spectra, *IEEE Trans. Geo. Rem. Sens.*, **33**, 4.

Hasselmann, K., and S. Hasselmann, 1991, On the nonlinear mapping of an ocean wave spectrum into a synthetic aperture radar image spectrum and its inversion, J. Geophys. Res, **96**(C6), 10713-10729.

Hasselmann, S., C. Brüning, K. Hasselmann and P. Heimbach, 1996, An improved algorithm for the retrieval of ocean wave spectra from SAR image spectra, *J. Geophys. Res.*, **101**, 16615-16629.

Krogstad, H.E. , 1992, A simple derivation of Hasselmann's nonlinear ocean-synthetic aperture radar transform, *J. Geophys. Res.,* **97** (C2), 2421-2425.

Mastenbroek C., and C.F. de Valk, 2000, A semi-parametric algorithm to retrieve ocean wave spectra from SAR, *J. Geophys. Res.*, **105**, (C2), 3947.

Tolman, H. L. , 2002, User manual and system documentation of WAVEWATCH-III version 2.22, *Tech. Rep.* 222, NOAA/NWS/NCEP/MMAB, Camp Springs, MD.